

Stabilities of the Aqueous Complexes $\text{Cm}(\text{CO}_3)_3^{3-}$ and $\text{Am}(\text{CO}_3)_3^{3-}$ in the Temperature Range 10–70 °C

Thomas Vercoeur,^{*,†,‡,§} Pierre Vitorge,^{*,†,‡} Badia Amekraz,[†] Eric Giffaut,[§] Solange Hubert,^{||} and Christophe Moulin[†]

CEA-DEN Saclay DPC/SECR/LSRM, 91191 Gif-sur-Yvette Cedex, France, Laboratoire Analyse et Environnement (CNRS-CEA-Université d'Evry UMR 8587), Université d'Evry-Val d'Essonne, bd F. Mitterrand, 91025 Evry, France, ANDRA, 1/7 rue Jean Monnet, 92298 Châtenay-Malabry Cedex, France, and Institut de Physique Nucléaire, IN2P3-CNRS, 91406 Orsay, France

Received February 8, 2005

The carbonate complexation of curium(III) in aqueous solutions with high ionic strength was investigated below solubility limits in the 10–70 °C temperature range using time-resolved laser-induced fluorescence spectroscopy (TRLFS). The equilibrium constant, K_3 , for the $\text{Cm}(\text{CO}_3)_2^- + \text{CO}_3^{2-} \rightleftharpoons \text{Cm}(\text{CO}_3)_3^{3-}$ reaction was determined ($\log K_3 = 2.01 \pm 0.05$ at 25 °C, $I = 3 \text{ M}$ (NaClO_4)) and compared to scattered previously published values. The $\log K_3$ value for Cm(III) was found to increase linearly with $1/T$, reflecting a negligible temperature influence on the corresponding molar enthalpy change, $\Delta_r H_3 = 12.2 \pm 4.4 \text{ kJ mol}^{-1}$, and molar entropy change, $\Delta_r S_3 = 79 \pm 16 \text{ J mol}^{-1} \text{ K}^{-1}$. These values were extrapolated to $I = 0$ with the SIT formula ($\Delta_r H_3^\circ = 9.4 \pm 4.8 \text{ kJ mol}^{-1}$, $\Delta_r S_3^\circ = 48 \pm 23 \text{ J mol}^{-1} \text{ K}^{-1}$, $\log K_3^\circ = 0.88 \pm 0.05$ at 25 °C). Virtually the same values were obtained from the solubility data for the analogous Am(III) complexes, which were reinterpreted considering the transformation of the solubility-controlling solid. The reaction studied was found to be driven by the entropy. This was interpreted as a result of hydration changes. As expected, excess energy changes of the reaction showed that the ionic strength had a greater influence on $\Delta_r S_3$ than it did on $\Delta_r H_3$.

1. Introduction

Safety assessments of possible underground repositories for high-level radioactive wastes require the prediction of the radiotoxicity induced by the release of radionuclides into natural aquifers.¹ The migration of radionuclides would be limited by their solubilities and interactions on inorganic materials (i.e., sorption) in the environment. Conversely aqueous complexation can increase their migration. Tremendous efforts have been made to acquire the data needed for modeling the aqueous speciation of the relevant radionuclides, typically actinides (An) and lanthanides (Ln). For equilibrated deep groundwaters, this modeling is based on the corresponding thermodynamic data: Gibbs energies of

reaction, $\Delta_r G$, or equivalently, equilibrium constants for a given temperature and pressure. Because of their important roles in underground water for f-block element ions, redox reactions, hydrolysis, and complexation reactions with carbonate have been the focus of major attention.² Several f-block elements are stable at the +3 oxidation state, typically the radioelements Am and Cm, as well as radionuclides of lanthanides, some of which are important fission products. Furthermore, the possible reduction of aqueous Pu(IV) to Pu(III) in chemical conditions of deep groundwaters cannot be excluded. We typically calculated the aqueous speciation at 25 °C in interstitial waters of clayey materials in the Callovo–Oxfordian formation, which is being studied as a possible disposal site for high-level radioactive wastes in France. According to the standard $\text{Pu}^{4+}/\text{Pu}^{3+}$ redox potential and formation constants selected by the Nuclear Energy Agency (NEA),³ Pu(III) would predominate in the reducing conditions of the groundwater⁴ ($E = -181 \text{ mV/SHE}$) at pH 7.3 and $I = 0.09 \text{ M}$ in the forms Pu^{3+} (32%), PuOH^{2+} (28%), $\text{Pu}(\text{OH})_2^+$ (21%), and PuCO_3^+ (19%).

* To whom correspondence should be addressed. Phone: +33-1-6908-3265. Fax: +33-1-6908-5411. E-mail: thomas.vercoeur@cea.fr (T.V.); pierre.vitorge@cea.fr (P.V.).

† CEA-DEN Saclay DPC/SECR/LSRM.

‡ Université d'Evry-Val d'Essonne.

§ ANDRA.

|| Institut de Physique Nucléaire (IPN).

(1) Hadermann, J. The Pillars of Safety. In *Modelling in Aquatic Chemistry*; Grenthe, I., Puidomech, I., Eds; Elsevier Science BV: Amsterdam, 1997.

(2) Clark, D. L.; Hobart, D. E.; Neu, M. P. *Chem. Rev.* **1995**, *95*, 25–48.

Thermochemical databases have been constructed from experimental data on An(III) and may also rely on analogies between Pu, Am, and Cm,^{3,5,6} as well as with Ln(III) for the missing thermodynamic data.^{7,8} However, a lack of measurements for the influence of temperature on aqueous speciation has been pointed out. In the early stage of the disposal, the radioactive decays can increase the temperature in the vicinity of the waste packages. Even though the storage should be designed to limit this temperature increase to about 90 °C, it is still useful to investigate the effects of temperature on the behaviors of An(III) and Ln(III) in carbonated aqueous solutions. Because the solubility of M³⁺ f-block element ions in such chemical systems at room temperature is usually lower than 10⁻⁴ M down to less than 10⁻⁸ M, formation constants of aqueous complexes were often derived from solubility measurements.^{5,9-15} At room temperature, it might be difficult to achieve equilibrium conditions within a reasonable amount of time, and a metastable solid phase of poor crystallinity might control the solubility. The determination of thermodynamic data for aqueous species equilibrated with metastable solid phases should still be relevant, even though scattering of data, as observed for the stability of the limiting carbonate complex, Am(CO₃)₃³⁻,^{5,15} may result from the difficulty in interpreting solubility measurements. At temperatures higher than room temperature, the thermodynamic interpretations of the experimental results were found to be complicated by crystallinity changes and other transformations of the solid phase, as observed for the Np(V)^{3,16,17} and Am(III) carbonate compounds.^{5,12,18} As there are very few published data about the temperature influence

on M³⁺ carbonate complexes, it seems reasonable to re-examine the available solubility data, typically the single-solubility study of Am(III) at elevated temperatures,¹² trying several possible interpretations. Other studies about the temperature influence on the formation of M³⁺ carbonate complexes have been performed below the solubility limits of Ln(III) or An(III) carbonate compounds. Cantrell et al. studied the carbonate complexation of Eu(III) using the solvent extraction method at pH < 7 with controlled CO₂- (g).¹⁹ From the slight increase of the stability constants in a quite restricted temperature range (15 to 35 °C), the formations of EuCO₃⁺, Eu(CO₃)₂⁻, and EuHCO₃²⁺ were found to be endothermic, and Δ_rH values were determined at 0.68 mol kg⁻¹ ionic strength. Wruck et al. studied the formation of AmCO₃⁺ between 25 and 75 °C using pulsed-laser photoacoustic spectroscopy.²⁰ The authors estimated the enthalpy of reaction at 0.1 mol kg⁻¹ ionic strength, on the basis of determinations at two temperatures, 25 and 50 °C. These results were fairly consistent with the Δ_rH value for the analogous EuCO₃⁺ compound, but they were not selected in the recent thermochemical database (TDB) of the OECD NEA (Organization for Economic Cooperation and Development, Nuclear Energy Agency) because of insufficient experimental details in the paper; the authors of the NEA-TDB argued that the series of spectra at elevated temperatures did not exhibit isobestic points as was expected.¹⁵

Calorimetry is widely used for measuring the enthalpy changes of reactions. Unfortunately, it is not sensitive enough for most of the carbonate complexes of Ln(III) and An(III) because they are formed in chemical conditions where their solubilities are too low. Alternatively, Δ_rH can be deduced from the dependency of the corresponding equilibrium constant, *K*, with temperature on the basis of the van't Hoff isochore (i.e., from the slope of the log *K* vs 1/*T* plot).²¹ This method has been applied to carbonate systems.^{19,20} As any slope analysis, it is less accurate than direct measurements; on the other hand, when the experimental determinations of *K* are associated with speciation measurements, this gives more confidence in the stoichiometry of the reactions used to interpret the experiments, a key problem for the carbonate complexes of Ln(III) and An(III).²² Time-resolved laser-induced fluorescence spectroscopy (TRLFS) has recently been used to study the formation of the carbonate complexes of the Eu³⁺ and Cm³⁺ ions at room temperature, below their solubility limits.²³⁻²⁶ There has been increasing interest in the capabilities of TRLFS for probing complexes of fluorescing f-block element ions, namely Eu³⁺, Cm³⁺, and UO₂²⁺, outside the 20–25 °C temperature range. High-

- (3) Lemire, R.; Fuger, J.; Nitsche, H.; Potter, P.; Rand, M.; Rydberg, J.; Spahiu, K.; Sullivan, J.; Ullman, W.; Vitorge, P.; Wanner, H. *Chemical Thermodynamics of Neptunium and Plutonium*; Elsevier BV: Amsterdam, 2001.
- (4) Gaucher, E.; Robelin, C.; Matray, J. M.; Négrel, G.; Gros, Y.; Heitz, J. F.; Vinsot, A.; Rebours, H.; Cassagnabère, A.; Bouchet, A. *Water Geochemistry and Hydrogeology* **2004**, *29*, 55–77.
- (5) Silva, R. J.; Bidoglio, G.; Rand, M. H.; Robouch, P. B.; Wanner, H.; Puigdomenech, I. *Chemical Thermodynamics of Americium*; Elsevier BV: Amsterdam, 1995; reprinted by NEA-OECD, <http://www.nea.fr/html/dbtdb/pubs/americium.pdf>
- (6) Vitorge, P.; Capdevila, H. *Radiochim. Acta* **2003**, *91*, 623–631.
- (7) Choppin, G. R. *J. Less-Common Metals* **1983**, *93*, 232–330.
- (8) Krauskopf, K. B. *Chem. Geol.* **1986**, *55*, 323–335.
- (9) Ferri, D.; Grenthe, I.; Hietanen, S.; Salvatore, F. *Acta Chem. Scand. A* **1983**, *37*, 359–365.
- (10) Robouch, P. Contribution à la prévision du comportement de l'américium, du plutonium et du neptunium dans la géosphère: données géochimiques. PhD Thesis, Université Louis Pasteur, Strasbourg, France, 1987.
- (11) Felmy, A. R.; Rai, D.; Fulton, R. W. *Radiochim. Acta* **1990**, *50*, 193–204.
- (12) Giffaut, E. Influence des ions chlorure sur la chimie des actinides. Effets de la radiolyse et de la température. PhD Thesis, Université Paris-sud, Orsay, France, 1994.
- (13) Runde, W.; Kim, J. I. Report RCM 01094; Technische Universität München; Munich, Germany, 1994; p 227 (in German).
- (14) Rao, L.; Rai, D.; Felmy, A. R.; Fulton, R. W.; Novak, C. F. *Radiochim. Acta* **1996**, *75*, 141–147.
- (15) Guillaumont, R.; Fanghänel, T.; Fuger, J.; Grenthe, I.; Neck, V.; Palmer, D. A.; Rand, M. H. *Update on the Chemical Thermodynamics of Uranium, Neptunium, Plutonium, Americium and Technetium*; Elsevier BV: Amsterdam, 2003.
- (16) Lemire, R. J.; Boyer, G. D.; Campbell, A. B. *Radiochim. Acta* **1993**, *61*, 57–63.
- (17) Vitorge, P.; Capdevila, H. Report CEA-R-5793; Commissariat à l'Energie Atomique: Saclay, France, 1998; p 147 (in French).
- (18) Vitorge, P. *Radiochim. Acta* **1992**, *58/59*, 105–107.

- (19) Cantrell, K. J.; Byrne, R. H. *J. Sol. Chem.* **1987**, *16*, 555–566.
- (20) Wruck, D. A.; Palmer, C. E. A.; Silva, R. J. *Radiochim. Acta* **1999**, *85*, 21–24.
- (21) Atkins, P. *The Elements of Physical Chemistry*, 3rd ed; Oxford University Press: Oxford, U.K., 2001.
- (22) Vercouter, T.; Vitorge, P.; Trigoulet, N.; Giffaut, E.; Moulin, C. *New J. Chem.* **2005**, *29*, 544–553.
- (23) Fanghänel, T.; Weger, H.; Könnecke, T.; Neck, V.; Paviet-Hartmann, P.; Steinle, E.; Kim, J. I. *Radiochim. Acta* **1998**, *82*, 47–53.
- (24) Fanghänel, T.; Könnecke, T.; Weger, H.; Paviet-Hartmann, P.; Neck, V.; Kim, J. I. *J. Solution Chem.* **1999**, *28*, 447–462.
- (25) Plancque, G.; Moulin, V.; Toulhoat, P.; Moulin, C. *Anal. Chim. Acta*, **2003**, *478*, 11–22.

temperature studies using TRLFS focused on the dependency of the fluorescence lifetimes on the temperature. The fluorescence properties of the hydroxides,^{27–30} sulfate complexes, and fluoride complexes²⁸ of UO_2^{2+} were determined, as well as those of the Eu^{3+} complexes.³¹ On the basis of speciation predictions, the lifetime, τ , of each species was deduced, and the expected Arrhenius law was verified for the dependency of τ on the temperature, enabling an estimation of activation energies. In recent studies, stability constants were determined by TRLFS at variable temperatures,^{32,33} but to our knowledge, no experiment has been carried out using this technique for carbonate complexation studies.

Many complexes with stoichiometries of $\text{Am}(\text{CO}_3)_i(\text{OH})_j^{3-2i-j}$ have been proposed for M^{3+} f-block elements to interpret experimental observations in $\text{OH}^-/\text{CO}_3^{2-}/\text{HCO}_3^-$ aqueous solutions at room temperature. Robouch was the first to show that the solubility of $\text{Am}_2(\text{CO}_3)_3(\text{s})$ at 25 °C only depends on $[\text{CO}_3^{2-}]$ for variable pH, which indicated that only carbonate complexes of Am(III) are formed.¹⁰ In addition to the discrepancies between published formation constants for carbonate complexes,^{5,15} there is still a debate on the limiting carbonate complex: $\text{M}(\text{CO}_3)_3^{3-}$ and $\text{M}(\text{CO}_3)_4^{5-}$ stoichiometries have been proposed for the An^{3+} and Ln^{3+} ions. We recently pointed out that the limiting complex is $\text{Eu}(\text{CO}_3)_3^{3-}$ in $\text{Na}^+/\text{CO}_3^{2-}$ aqueous solutions, while $\text{M}(\text{CO}_3)_4^{5-}$ stoichiometry has been demonstrated for $\text{M}^{3+} = \text{Ce}^{3+}$, a large lanthanide ion, in the same $\text{Na}^+/\text{CO}_3^{2-}$ conditions and for $\text{M}^{3+} = \text{Eu}^{3+}$ in chemical conditions where Na^+ was replaced with K^+ .²² These stoichiometries were essentially evidenced by classical slope analysis of the solubility measurements because the shapes of the solubility curves are clearly different for the $\text{M}(\text{CO}_3)_3^{3-}$ and $\text{M}(\text{CO}_3)_4^{5-}$ predominant stoichiometries. By the same data treatment, the stoichiometry of the Am(III) limiting complex was also shown to be $\text{Am}(\text{CO}_3)_3^{3-}$ during solubility measurements in $\text{Na}^+/\text{CO}_3^{2-}$ aqueous solutions at room temperature,^{10,12,13} and this was qualitatively confirmed by spectrophotometry.¹⁰ For this reason, in $\text{Na}^+/\text{CO}_3^{2-}$ aqueous solutions, we expect the $\text{M}(\text{CO}_3)_3^{3-}$ stoichiometry for the limiting complexes of Ln^{3+} and An^{3+} ions at least smaller (or equivalently heavier) than Eu^{3+} and Am^{3+} . Consequently, the expected stoichiometry of the limiting carbonate complex for Cm^{3+} is $\text{Cm}(\text{CO}_3)_3^{3-}$.

in such ionic conditions, although this stoichiometry disagrees with the interpretation of TRLFS data for NaCl solutions at 25 °C which used a limiting complex of $\text{Cm}(\text{CO}_3)_4^{5-}$ stoichiometry.^{23,24}

To decrease the scattering of the published values for the formation constant of $\text{Cm}(\text{CO}_3)_3^{3-}$ at 25 °C and to determine the corresponding $\Delta_r H$, we report in this paper the first determination of equilibrium constants for carbonate complexes of Cm(III) in the 10–70 °C temperature range using TRLFS. This study was focused on the formation of $\text{Cm}(\text{CO}_3)_3^{3-}$ in aqueous solutions, mainly at high ionic strength, 3 M Na^+ , with CO_3^{2-} concentrations higher than 10^{-3} M. The choice of these conditions was motivated by (i) the possibility of studying solutions in which only two species, $\text{Cm}(\text{CO}_3)_2^-$ and $\text{Cm}(\text{CO}_3)_3^{3-}$, are formed, thereby avoiding mixtures of too many species that might have altered the selectivity of the technique; (ii) the easier control of the carbonate speciation, particularly the possible changes of P_{CO_2} when varying the temperature, which could modify the CO_3^{2-} concentration; and (iii) the high fluorescence yield of $\text{Cm}(\text{CO}_3)_3^{3-}$ that was detected even at concentrations lower than 3×10^{-8} M. We also reinterpreted the solubility measurements of Am(III) in 4 M NaCl solutions between 20 and 70 °C from data that only appeared in Giffaut's thesis¹² to compare with the dissociation of analogous $\text{Am}(\text{CO}_3)_3^{3-}$ and to choose between the scattered published values for its stability. The influence of the temperature on equilibrium constants is finally discussed to evidence whether the stepwise formation reaction of the limiting carbonate complex is enthalpy or entropy driven, and it is compared with the thermodynamic data for other systems.

2. Experimental Section

2.1. Materials. Millipore deionized water (Alpha-Q, 18.2 MΩ cm) was used throughout the preparations. All the curium solutions were prepared by dilution of a ²⁴⁸Cm solution in 0.1 M HNO_3 with a concentration of 4.54×10^{-6} M, measured by inductively coupled plasma mass spectrometry. $\text{NaClO}_4 \cdot \text{H}_2\text{O}$ (>99.0%) and anhydrous Na_2CO_3 (>99.8%) were purchased from Merck (R. P. Normapur), and NaHCO_3 (100.0%) was purchased from Sigma; they were used without further purification. Specified gas mixtures were obtained from Messer (CO_2/Ar 100.0/0.0 and 10.0/90.0).

2.2. Preparation Procedure. Small volumes of the ²⁴⁸Cm stock solution were added to NaHCO_3 and Na_2CO_3 solutions, so that the Cm concentration ranged between 2.27×10^{-8} and 2.42×10^{-8} M and was sufficiently low to prevent precipitation. NaClO_4 salt was used to fix the Na^+ concentration at 3 M. In one of the bicarbonate solutions, the pH was lowered by bubbling a 10% CO_2 gas mixture that was first passed through a NaClO_4 solution with the same ionic strength (3 M) to saturate the gas with water. The CO_2 partial pressure was calculated in the same manner as in Spahiu's work,³⁴ $P_{\text{CO}_2} = (P_{\text{T}} - P_{\text{H}_2\text{O}})x_{\text{CO}_2}$, where P_{T} is the total pressure inside the glovebox in which experiments were performed, $P_{\text{H}_2\text{O}}$ is the water vapor pressure at 23 °C,³⁵ and $x_{\text{CO}_2} = 0.1$.

(26) Vercouter, T.; Amekraz, B.; Moulin, C.; Vitorge, P. Lanthanide and actinide inorganic complexes in natural waters: TRLFS and ESI-MS studies. In *International Conference Atalante 2004: Advances for Future Nuclear Fuel Cycles*; Commissariat à l'Énergie Atomique, Unité de Communication et Affaires Publiques: Bagnols-sur-Cèze, France, 2004; O22–02.

(27) Eliet, V.; Grenthe, I.; Bidoglio, G. *Appl. Spectrosc.* **2000**, *54*, 99–105.

(28) Kimura, T.; Nagaiishi, R.; Ozaki, T.; Arisaka, M.; Yoshida, Z. *J. Nucl. Sci. Techn.* **2002**, *Supplement 3*, 233–239.

(29) Kirishima, A.; Kimura, T.; Tochiyama, O.; Yoshida, Z. *J. Alloys Compd.* **2004**, *374*, 277–282.

(30) Zanonato, P. L.; Di Bernardo, P.; Bismondo, A.; Liu, G.; Chen, X.; Rao, L. *J. Am. Chem. Soc.* **2004**, *126*, 5515–5522.

(31) Kimura, T.; Nagaiishi, R.; Arisaka, M.; Ozaki, T.; Yoshida, Z. *Radiochim. Acta* **2002**, *90*, 715–719.

(32) Yeh, M.; Riedener, T.; Bray, K. L.; Clark, S. B. *J. Alloys Compd.* **2000**, *303–304*, 37–41.

(33) Colette, S.; Amekraz, B.; Madic, C.; Berthon, L.; Cote, G.; Moulin, C. *Inorg. Chem.* **2004**, *43*, 6745–6751.

(34) Spahiu, K. Carbonate complex formation in lanthanoid and actinoid systems. PhD Thesis, The Royal Institute of Technology, Stockholm, Sweden, 1983.

(35) International Association for the Properties of Water and Steam. *Release on the IAPWS Industrial Formulation 1997 for the Thermodynamic Properties of Water and Steam*; IAPWS Secretariat, Electric Power Research Institute: Palo Alto, CA, 1997.

2.3. [H⁺] Measurements and Carbonate Speciation. [H⁺] was measured inside the fluorescence cells using combined glass microelectrodes (Radiometer Analytical, XC161). The KCl solutions in the reference compartments were replaced with a solution composed of 2.99 or 0.09 M NaClO₄ and 0.01 M NaCl to avoid KClO₄ precipitation at the electrode liquid junction. Each electrode was calibrated at 23 ± 1 °C with a 0.01 M HCl solution, a 0.1 M NaHCO₃ solution equilibrated with 100% CO₂ gas, and an equimolar Na₂CO₃/NaHCO₃ solution, all containing appropriate amounts of NaClO₄ to keep [Na⁺] constant at 3 (−log [H⁺] = 2.00, 7.00, and 9.61, respectively) and 0.1 M (−log [H⁺] = 2.00, 6.63, and 9.90, respectively). The H⁺ concentrations in these standard solutions were calculated with the specific ion interaction theory (SIT) formula using equilibrium constants and SIT parameters for the protonations of CO₃^{2−} from ref 3 (the SIT parameters are given at 25 °C, but the temperature difference led to negligible corrections) and is given as Supporting Information (Table S1). The slope of the electrode was typically higher than 98% of the theoretical slope for each calibration. Measurements were performed using a modified electrode that had the same [Na⁺] as the solution in which the −log [H⁺] values were measured.

Potentiometric measurements were only performed at 23 ± 1 °C to avoid calibrations at different temperatures that could introduce systematic errors in the −log [H⁺] values and to limit the perturbation of the solutions, particularly CO₂(g) leakage when opening the cell. Because the working solutions were actually buffers, the numbers of moles of HCO₃[−] and CO₃^{2−} did not vary with temperature, and this was used to calculate the corresponding concentrations at each temperature. So [HCO₃[−]] and [CO₃^{2−}] were only corrected for volume variations using the thermal dilatation coefficients for NaCl solutions³⁶ (Table S2 of the Supporting Information), which were assumed to be representative of the NaClO₄ solutions. These corrections were lower than 0.02 log units on the concentration values.

2.4. Temperature Cycles. The temperature of the solution in the fluorescence cell was controlled by circulating water through the cell support from a constant-temperature bath. For each temperature, the solution was equilibrated for at least 20 min, which was sufficient to reach stable temperature in every condition. For a given temperature of the circulating water, the actual temperature of the solution in the cell was estimated by measuring them in a curium-free solution. The uncertainty was estimated to be ±0.5 °C. After the −log [H⁺] values were measured at 23°C, the solution underwent a temperature cycle: typically, it was first equilibrated at 25 °C, then cooled to 10 °C, and heated to 37, 50, and 70 °C; the cycle was ended after the solution was equilibrated again at 25 °C to ensure that the fluorescence spectrum had not changed.

2.5. Time-Resolved Laser-Induced Fluorescence Spectroscopy. The fluorescence was induced by a Nd:YAG Laser delivering a 6 mJ pulsed laser beam at 355 nm. The laser beam was driven into the quartz cell placed in a glovebox through two lenses that focused and shaped the beam with an optimized geometry. The emitted light was collected using a combination of mirrors and lenses in a spectrometer with a 600 mm^{−1} grating (Roper Scientific). Fluorescence was detected using a CCD camera cooled to −18 °C providing fluorescence spectra with a resolution of 0.2 nm. The fluorescence signal was increased by the use of two spherical mirrors in the cell support that reflected the laser and the fluorescence lights.

The fluorescence spectra were recorded with constant gate delay (10 μs) and gate width (600 μs) to collect the largest part of the fluorescence that was emitted by Cm(III). Fluorescence lifetimes were derived from the decay of the intensity measured by varying the gate delay for a constant gate width (50 μs). The decay curves were fitted with monoexponential functions so that average values of the lifetimes were obtained. Uncertainties of 10% were assigned to the fluorescence intensity on the basis of expected errors on the curium concentrations in relation to dilution and possible sorption of Cm(III) on the wall of the quartz cell, as already observed in similar experiments.²³ As the curium concentration was very low, even the removal of small amounts of Cm(III) from the bulk solution could be significant. Consequently, the cells containing the solution were gently shaken just before they were placed in the cell support for better homogenization, except when the solution was equilibrated with CO₂(g).

2.6. Solubility Measurements of Am(III). The experimental details described in Giffaut's thesis¹² are outlined here. Am₂(CO₃)₃(s) was prepared under 1 atm CO₂(g) for 10 days at pH 7.2 and partially dissolved into Na⁺/HCO₃[−]/CO₃^{2−} solutions with 4 M NaCl. Radiolytic oxidation of Am(III) into Am(V) due to the high Cl[−] concentration³⁷ was observed at first, and Fe(s) powder was added to the mixture to obtain reducing conditions. The solubility of Am(III) in a few Na⁺/HCO₃[−]/CO₃^{2−} solutions with 0.1 M NaCl, where no oxidation into Am(V) was expected, was not altered by the presence of Fe(s): although iron compounds may have formed, no evidence of a coprecipitation with Am(III) was found. Thus, it was assumed that the Am(III) solubility was controlled by a solid phase of Am(III) in the 4 M NaCl solutions with no significant effect of any Fe compound. The under-saturated batch solutions were heated at 70 °C, which was the initial temperature of the cycle. The solubility was followed with time: the shape of the experimental solubility curves vs [CO₃^{2−}] showed a solid-phase transformation, and the slope analysis was consistent with the formation of NaAm(CO₃)₂(s) for [CO₃^{2−}] > 0.01 M. Equilibration lasted 8 weeks to allow complete phase transformation at 70 °C and to achieve equilibrium conditions. The temperature was then varied from 70 to 20 °C by 10 °C steps, and then back up from 20 to 70 °C to ensure that equilibrium had been obtained in all conditions. All of the batches were continuously stirred. The temperature was controlled within ±1 °C. Aliquots of solutions were taken out and filtered using 0.22 μm porosity filters because it was verified that this pore size ensured efficient filtration. The ²⁴¹Am concentrations in the filtrates were measured by α counting (LKB 1219) with a reproducibility better than 8%. [H⁺] was measured using glass combined electrodes (Tacussel, XC111) with a 4 M NaCl solution in the compartment of the Ag/AgCl reference electrode. Calibration was performed at each temperature with the following standard solutions at I = 4 M: (i) 0.05 M Na₂CO₃, 0.05 M NaHCO₃, and 3.81 M NaCl; (ii) 0.025 M KH₂PO₄, 0.025 M Na₂HPO₄, and 3.905 M NaCl; and (iii) 0.001 M HCl and 4 M NaCl. The pK_a of the buffers were estimated for the different temperatures and 4 M NaCl ionic medium.

3. Treatment of Data

3.1. Fitting of the Fluorescence Measurements. The treatment of the spectroscopic data was based on the decomposition of the measured fluorescence spectra into reference spectra corresponding

(36) Puigdomenech, I.; Plyasunov, A. V.; Rard, J. A.; Grenthe, I. Temperature Correction to Thermodynamic Data and Enthalpy Calculations. In *Modelling in Aquatic Chemistry*; Grenthe, I., Puigdomenech, I., Eds; NEA/OECD: Paris, 1997; Chapter X.

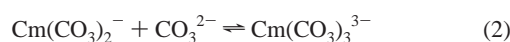
(37) Giffaut, E.; Vitorge, P. Evidence of radiolytic oxidation of ²⁴¹Am in Na⁺/Cl[−]/HCO₃[−]/CO₃^{2−} media. In *Scientific Basis for Nuclear Waste Management XVI*, Proceedings of the MRS 92 Fall meeting, Boston, 30 Nov–5 Dec 1992; Interrante, C., Pabalan, R., Eds; Materials Research Society: Warrendale, PA, 1993; pp 747–751.

to individual curium species. In this study, we focused on the dissociation of the limiting carbonate complex of Cm(III), Cm(CO₃)₃³⁻. The most relevant equation is given here since the sensitivity analysis of our data toward speciation models showed that Cm(CO₃)₃³⁻ likely dissociated into only Cm(CO₃)₂⁻; it will be shown below that the dissociation of the limiting complex actually corresponds to the loss of one carbonate ion, without any OH⁻ or H⁺ involved in the dissociation reaction. For a given wavelength, λ , the corresponding equation for fitting experimental fluorescence measurements, $F_{\text{mes},\lambda}$, is

$$\frac{F_{\text{mes},\lambda}}{[\text{Cm}]_{\text{T}}} = \frac{F_{2,\lambda} + F_{3,\lambda}K_3[\text{CO}_3^{2-}]}{1 + K_3[\text{CO}_3^{2-}]} \quad (1)$$

The molar fluorescence intensities, $F_{2,\lambda}$, and $F_{3,\lambda}$, correspond to the intensities at wavelength λ for solutions of pure Cm(CO₃)₂⁻ and Cm(CO₃)₃³⁻, respectively. For each temperature, the stepwise formation constant, K_3 , was fitted to the $F_{\text{mes},\lambda}$ data in the range of wavelengths where fluorescence was detected (i.e., 580–630 nm). A range of acceptable $\log K_3$ values was determined by examination of the standard deviation of the fit to assess the uncertainties of $\log K_3$: the uncertainties were taken to cover this interval.

3.2. Thermodynamic Data. The dissociation of the limiting carbonate complex of Cm(III) was described by the equilibrium



with the equilibrium constant

$$K_3 = \frac{[\text{Cm}(\text{CO}_3)_3^{3-}]}{[\text{Cm}(\text{CO}_3)_2^-][\text{CO}_3^{2-}]} \quad (3)$$

When the ionic strength was fixed (typically at 3 M), the activity coefficients remained constant, and no correction was required, namely, the three terms were constant in

$$\log K_3^\circ(T) = \log K_{3,\text{m}}(T) + \Delta_r \log \gamma_3(T) \quad (4)$$

where $^\circ$ denotes the reference state (zero ionic strength), the subscript m denotes the molality scale (mol kg⁻¹), and $K_{3,\text{m}}$ is related to K_3 through molal-to-molar conversion factors.¹⁵ For different ionic conditions, we used a simple SIT formula to calculate

$$\Delta_r \log \gamma_3(T) = -4D(T) + \Delta\epsilon_3(T)I_{\text{m}} \quad (5)$$

where $D(T) = A(T)I_{\text{m}}^{1/2}/(1 + a_j B(T)I_{\text{m}}^{1/2})$ is a Debye–Hückel term, I_{m} is the ionic strength (mol kg⁻¹), $\Delta\epsilon_3$ is the difference of empirical ion pair coefficients (kg mol⁻¹).³ $D(T^\circ)$, the value at the temperature 298.15 K, was calculated with the usual parameters $A(T^\circ) = 0.509$ kg^{1/2} mol^{-1/2}, $a_j B(T^\circ) = 1.5$ kg^{1/2} mol^{-1/2} at 1 bar.³ For ionic strength corrections at temperatures different from 25 °C, the parameters were calculated as follows: second-order polynomial equations were fitted to tabulated values of $A(T)$ and $B(T)$,³ and no temperature dependency was assumed for a_j , which was calculated as $a_j = 1.5/B(T^\circ) = 1.5/0.3284 = 4.568$ Å. The calculated values are reported in Table S3 of the Supporting Information. $\Delta\epsilon_3(T^\circ) = -0.02 \pm 0.04$ kg mol⁻¹ was calculated from the individual ϵ values for Am(III) at 25 °C.⁵ The temperature influence on $\Delta\epsilon_3$ is not known; however in theory, $\Delta\epsilon(T) = \Delta\epsilon(T^\circ)T^\circ/T$ because $\Delta\epsilon(T)I_{\text{m}}$ is a second virial expansion term. This correction was less than 0.003 kg mol⁻¹ for $\Delta\epsilon_3$ in the temperature range of 10–70 °C and was therefore neglected: for calculating the value of $\Delta_r \log \gamma_3(T)$, we used the constant value $\Delta\epsilon_3(T) = -0.02 \pm 0.04$ kg mol⁻¹ (i.e., only $D(T)$ varied with T in eq 5 for ionic strength corrections).

The enthalpy and heat capacity changes for reaction 2 were deduced from the integration of the van't Hoff isochore.²¹ In model A, the enthalpy variation $\Delta_r H_3$ was assumed to be temperature independent

$$\log K_3(T) = \log K_3(T^\circ) - \frac{\Delta_r H_3(T^\circ)}{r} \left(\frac{1}{T} - \frac{1}{T^\circ} \right) \quad (6)$$

where $r = R \ln 10 = 19.14487 \pm 0.00016$ J K⁻¹ mol⁻¹ and R is the molar gas constant. In model B, the heat capacity change, $\Delta_r C_{\text{p}3}$, was assumed to be constant

$$\log K_3(T) = \log K_3(T^\circ) - \frac{\Delta_r H_3(T^\circ)}{r} \left(\frac{1}{T} - \frac{1}{T^\circ} \right) + \frac{\Delta_r C_{\text{p}3}(T^\circ)}{r} \left(\frac{T^\circ}{T} - 1 + \ln \frac{T}{T^\circ} \right) \quad (7)$$

Note that, in this case, $\Delta_r H_3$ varies linearly with temperature and

$$\left(\frac{T^\circ}{T} - 1 + \ln \frac{T}{T^\circ} \right) \approx \frac{1}{2} \left(\frac{T^\circ}{T} \right)^2$$

therefore the last term is a second-order term. Both models were tested on the experimental data.

The ionic strength influences on the thermodynamic functions, $\Delta_r H_3$ and $\Delta_r S_3$, are the excess enthalpy change

$$\Delta_r H^{\text{ex}} = -rT^2 \left(\frac{\partial \Delta_r \log \gamma}{\partial T} \right)_P \quad (8)$$

and the excess entropy change

$$\Delta_r S^{\text{ex}} = -r \left(\Delta_r \log \gamma + T \left(\frac{\partial \Delta_r \log \gamma}{\partial T} \right)_P \right) \quad (9)$$

respectively,³⁷ which are also temperature (and pressure, P) dependent. Thus, the neglect of the temperature influence on $\Delta_r \log \gamma$ is equivalent to neglecting $\Delta_r H^{\text{ex}}$ and the ionic strength corrections on $\Delta_r H$, an usual approximation assuming only entropic ionic strength corrections on equilibrium constants.³ According to eq 5 and assuming that the temperature dependency of $\Delta\epsilon_3$ is negligible,

$$\left(\frac{\partial \Delta_r \log \gamma_3}{\partial T} \right)_P \approx -4 \left(\frac{\partial D(T)}{\partial T} \right)_P \quad (10)$$

the values of which are calculated from Table S3 of the Supporting Information.

4. Results and Discussion

4.1. Spectroscopic Features of Cm(III). The fluorescence of Cm(III) in aqueous solution corresponds to the transition from the lowest excited state, A, to the ground state, Z. Strong spin–orbit coupling mixes several spectroscopic terms among which the most significant contributions are from ⁸S_{7/2} for Z, ⁶P_{7/2}, and ⁶D_{7/2} for A.^{38–40} Depending on the symmetry of the Cm³⁺ surrounding and the strength of chemical bonds, both states can split into several ligand-field components. However, in aqueous solutions, the ligand-field splitting is

(38) Carnall, W. T.; Rajnak K. *J. Chem. Phys.* **1975**, *63*, 3510–3514.

(39) Beitz, J. V. *Radiochim. Acta* **1991**, *52/53*, 35–39.

(40) Hubert, S.; Edelstein, N. M. Actinide Compounds: Optical Properties. In *Encyclopedia of Materials: Science and Technology*; Buschow, K. H. J., Cahn, R. W., Flemings, M. C., Ilshner, B., Kramer, E. J., Mahajan, S., Eds; Elsevier Science Ltd: New York, 2001; pp 18–22.

Table 1. Chemical Conditions of the TRLFS Measurements at 25 °C

solution label	I_m (mol kg ⁻¹)	$-\log [\text{H}^+]$	$\log [\text{CO}_3^{2-}]$	$\log [\text{HCO}_3^-]$	$\log P_{\text{CO}_2}$	$\tau^b/\mu\text{s}(N_{\text{H}_2\text{O}})$
b0	0.10	8.93	-2.07	-1.08	-2.38	98 (5.8)
B1	3.48	7.96	-2.71	-1.06	-1.02 ^a	
B2	3.52	8.57	-2.70	-1.66	-2.23	107 (5.2)
B3	3.48	9.05	-1.75	-1.19	-2.24	
B4	3.42	9.62	-1.30	-1.31	-2.94	189 (2.6)
C1	3.48	10.40	-1.84	-2.63	-5.03	
C2	3.48	10.60	-1.53	-2.52	-5.12	
C3	3.49	10.80	-1.02	-2.21	-5.01	
C4	3.48	10.95	-0.81	-2.15	-5.10	
C5	3.49	11.17	-0.51	-2.07	-5.24	
C6	3.49	11.54	-0.01	-1.94	-5.47	197 (2.5)
C7	4.93	11.95	0.30	-1.98	-5.68	

^a Bubbling of 10% CO₂(g). ^b Values are $\pm 10 \mu\text{s}$.

not resolved at room temperature. When Cm³⁺ is coordinated, fluorescence is shifted toward the red wavelengths as a result of the increased splitting which lowers the energy gap between Stark levels of the excited and ground states; the fluorescence peak of a Cm(III) complex in solution is usually large with shoulders. Small temperature variations (i.e., between 10 and 70 °C) may have some effects on spectroscopy in addition to changes in the aqueous speciation. First, increasing the temperature will lower the intensities of the radiative transitions in favor of nonradiative decays. Temperature changes may also slightly affect the populations of the vibronic and electronic levels. This effect was evaluated using energy gaps related to Cm³⁺ in LaCl₃ and ThO₂ host crystals,⁴⁰ giving weak and strong crystal fields, respectively. The population changes in both cases were assessed by calculating the occupation rates of the levels at 10 and 70 °C. Values were obtained by comparing kT (k is the Boltzmann constant) with the energy gap between a given Stark level and the lowest one using a Boltzmann distribution. Such a temperature range was concluded to have no significant effect on the population of the levels of the ground state since the ⁸S_{7/2} splitting is very weak. In addition, the occupation rate of the lowest level of the A state would vary from 0.74 to 0.70 for Cm³⁺/LaCl₃ and from 0.82 to 0.78 for Cm³⁺/ThO₂ in this temperature interval; the population change is even less when considering other compounds with different crystal field characteristics.⁴⁰ Thus, each component of the fluorescence peak should be slightly broadened when the temperature is increased, and the overall fluorescent peak should be slightly modified. Consequently, minor changes on the spectroscopic fingerprints of each complex are expected over the range of 10–70 °C, so that the identification of each species by TRLFS is made easier, allowing the speciation analysis.

4.2. Carbonate Complexes at 25 °C. The chemical conditions used for the TRLFS measurements at 25 °C are reported in Table 1. Fluorescence was unchanged when [CO₃²⁻] was higher than 0.1 M (i.e., for solutions C3–C7) (Figure 1a). The maximum of the peak was found at 607.4 nm. When [CO₃²⁻] was lower than 0.1 M, the fluorescence peak decreased, and its maximum was shifted to 606.1 nm for solution B2, which was interpreted as dissociation of the limiting carbonate complex Cm(CO₃)₃³⁻ into Cm(CO₃)₂⁻. The loss of a single CO₃²⁻ in the dissociation reaction was supported by the examination of the shapes of the curves

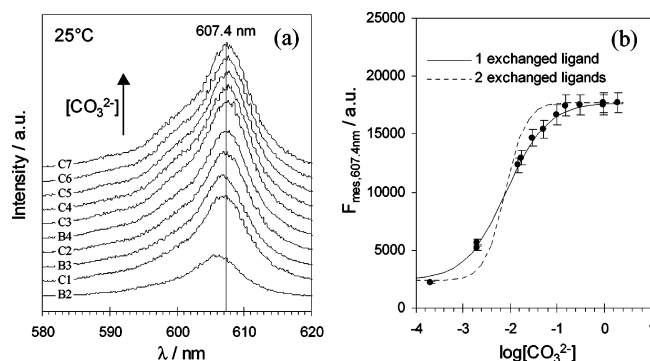


Figure 1. [CO₃²⁻] influence on the speciation of Cm(III) in bicarbonate and carbonate solutions at $I = 3 \text{ M}$ and 25 °C. (a) Fluorescence spectra corresponding to the solutions whose labels are indicated on the graphic, referring to Table 1. (b) Fluorescence intensities at 607.4 nm, the wavelength of the maximum intensity for Cm(CO₃)₃³⁻, over $\log[\text{CO}_3^{2-}]$. The curves were adjusted considering the exchange of 1 (solid line) and 2 (dashed line) ligands and gave evidence of the exchange of one CO₃²⁻ in the dissociation reaction.

which were fitted to the intensities at 607.4 nm (Figure 1b). The present interpretation was also supported by the $\log K_3$ values as discussed below. The fluorescence spectrum of Cm(CO₃)₃³⁻ was directly measured, whereas the one for Cm(CO₃)₂⁻, as well as $\log K_3$, was deduced from spectral decomposition. The value $\log K_3 = 2.08 \pm 0.10$ was obtained from reaction 2 at $I = 3 \text{ M}$, where the uncertainty accounted for both the experimental errors on the intensities and the possible minor formation of CmCO₃⁺ (expected to be less than 5% according to analogous Am(III) data⁵). The validity of the speciation model (i.e., sensitivity analysis for the formation of Cm(CO₃)₂⁻) was checked by comparing the spectra measured for a given ratio $R = [\text{Cm}(\text{CO}_3)_3^{3-}]/[\text{Cm}(\text{CO}_3)_2^-]$ ($= [\text{CO}_3^{2-}]K_3$) but different chemical conditions ($-\log [\text{H}^+] = 7.96$ and 8.57 and $I = 0.1$ and 3 M) (Figure 2). We chose the value $R = 0.22 \pm 0.02$ corresponding to $\log R = -0.66 \pm 0.04$ and $72 \pm 3\%$ of Cm(CO₃)₂⁻ and $28 \pm 3\%$ of Cm(CO₃)₃³⁻. Solution B1 was prepared by bubbling a 10% CO₂ gas mixture into a 0.1 M NaHCO₃ solution with $I = 3 \text{ M}$ in order to keep [CO₃²⁻] the same as in B2 but at a lower $-\log [\text{H}^+]$ value of 7.96. The pH change had no significant influence on the spectrum, which confirmed that under these conditions no exchange of H⁺ or OH⁻ was involved in the reaction, in agreement with reaction 2. Solution b0 was a 0.1 M NaHCO₃ solution without NaClO₄. According to $\log K_3(0.1 \text{ M}) = 1.37 \pm 0.10$ calculated from the extrapolation of $\log K_3(3 \text{ M}) = 2.08 \pm 0.10$ to $I = 0.1$

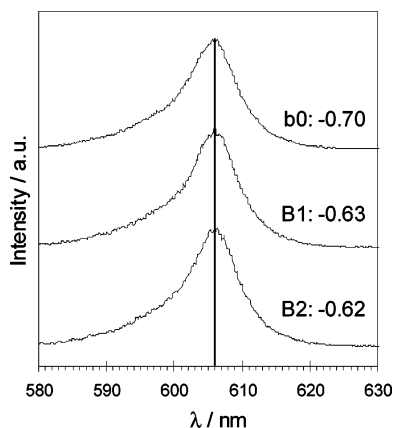


Figure 2. Sensitivity analysis for $\text{Cm}(\text{CO}_3)_2^-$ formation at 25 °C. The value at $I = 3 \text{ M}$, $\log K_3 = 2.08$, was used to calculate the values of $\log ([\text{CO}_3^{2-}] K_3)$ written on the figure, while $[\text{CO}_3^{2-}] K_3 = [\text{Cm}(\text{CO}_3)_3^{3-}]/[\text{Cm}(\text{CO}_3)_2^-]$. These values are similar for the solutions b0, B1, and B2 (Table 1). The spectra are identical, although different values were measured for the pH of solutions B1 and B2 ($-\log [\text{H}^+] = 7.96$ and 8.57 , respectively). This shows no influence of $[\text{OH}^-]$. Similarly the spectrum for b0 at $I = 0.1 \text{ M}$ is identical to the other ones, which were obtained at higher ionic strength ($I = 3 \text{ M}$), in agreement with the corresponding ionic strength corrections calculated using eqs 4 and 5.

M with eqs 4 and 5, the same speciation as in B2 was expected in b0 (virtually the same R value). This was confirmed by the similarity of the spectra shown in Figure 2.

In a 1 M Na_2CO_3 solution (C6), the fluorescence decreased with time as a monoexponential function. The corresponding lifetime, τ , was found to be $197 \pm 10 \mu\text{s}$, that value was then assigned to $\text{Cm}(\text{CO}_3)_3^{3-}$. This lifetime has the same order of magnitude as the ones measured in similar conditions by various authors; the values of 160,³⁹ 215,⁴¹ and $230 \mu\text{s}$ ²³ were typically measured in 1 M Na_2CO_3 . In a previous work, Decambox et al. reported values of 200 and $240 \mu\text{s}$ measured in 1 M K_2CO_3 solutions for the excitation wavelengths 337 and 385 nm, respectively.⁴² These values are also inside the range of 160–240 μs even if the formation of the tetracarbonato complex, $\text{Cm}(\text{CO}_3)_4^{5-}$, can be suspected in K^+ media, as observed for lanthanides.²²

The average number of remaining water molecules in the first hydration sphere of the Cm(III) triscarbonato species was calculated, using the Kimura's relationship,⁴³ to be 2.5 ± 0.5 from the lifetime ($197 \pm 10 \mu\text{s}$) measured in 1 M Na_2CO_3 solution. As CO_3^{2-} is expected to be a bidentate ligand toward the Cm^{3+} ion, the $[\text{Cm}(\text{CO}_3)_3(\text{H}_2\text{O})_{2.5}]^{3-}$ stoichiometry would result in the average coordination number 8.5 ± 0.5 , which is a little lower than 9.2 ± 0.5 , the value that has been estimated for the aquo Cm^{3+} ion.⁴³ The lifetime measured at 25 °C for solution B2 would suggest 5.2 ± 0.5 for the average number of remaining water molecules (Table 1). We estimated that it corresponded to 5.8 ± 1.0 water molecules in the first hydration shell of $\text{Cm}(\text{CO}_3)_2^-$ according to the relative ratio of each species

(41) Kim, J. I.; Klenze, R.; Wimmer, H.; Runde, W.; Hauser, W. *J. Alloys Compd.* **1994**, 213/214, 333–340.

(42) Decambox, P.; Mauchien, P.; Moulin, C. *Radiochim. Acta* **1989**, 48, 23–28.

(43) Kimura, T.; Choppin, G. R. *J. Alloys Compd.* **1994**, 213/214, 313–317.

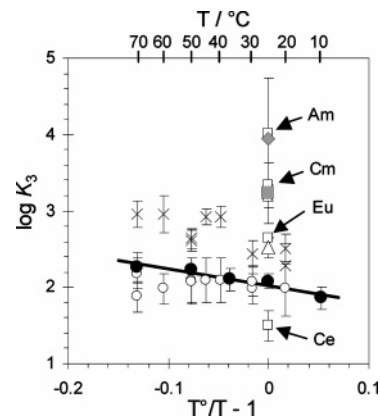


Figure 3. Comparison of $\log K_3$ values at various temperatures for Am(III) and Ln(III). K_3 values were corrected to $I = 3 \text{ M NaClO}_4$ with the SIT formula (eqs 4 and 5). TRLFS data for Cm(III) from this work (●) (Table 2); Am(III) solubility data obtained in 3 M NaClO_4 ¹⁰ (Δ), in 4 M NaCl media¹² (×), and our reinterpretation (○); selected constants for Am(III)⁵ (◆) and for Am/Cm(III)¹⁵ (■); literature data for Am(III),¹¹ Cm(III),^{23,24} Ce(III),⁹ and Eu⁴⁴ (□) as indicated on the graphic.

in these solutions, $R \approx 0.24$. This calculation suggested that the average stoichiometry is $[\text{Cm}(\text{CO}_3)_2(\text{H}_2\text{O})_{5.8}]^-$ and that the coordination number is 9.8 ± 1.0 , which has a large uncertainty and is in agreement with the estimated value for the aquo ion. It should also be noted that the coordination number of the $\text{Cm}(\text{CO}_3)_3^{3-}$ complex may be lowered by steric hindrance, even though this is not clearly evidenced by the lifetime measurements because of the large uncertainties.

From spectra at 25 °C, we obtained $\log K_3 = 2.08 \pm 0.10$, leading to $\log K_3^0 = 0.94 \pm 0.24$ after correction to $I = 0$ using eqs 4 and 5. This result has been compared with all the available $\log K_3$ values measured at room temperature for trications of various f-block elements: Ce(III),⁹ Eu(III),⁴⁴ Am(III),^{10–12} and Cm(III).^{23,24} These data have been corrected to $I = 3 \text{ M}$ (NaClO_4) using eqs 4 and 5 and plotted in Figure 3 (for $T^\circ/T - 1 = 0$).

$\text{Ce}(\text{CO}_3)_3^{3-}$ was observed to be less stable since $\log K_3 = 1.5 \pm 0.2$ ⁹ was lower than $\log K_3 = 2.08 \pm 0.10$ at $I = 3 \text{ M}$ (NaClO_4). We have already pointed out that Ce(III) has a different behavior than that of the smaller f-block element ions as it can actually form $\text{Ce}(\text{CO}_3)_4^{5-}$; a difference in $\log K_3$ was therefore not unexpected. A solvent extraction study also provided stability constants for $\text{Eu}(\text{CO}_3)_3^{3-}$ and $\text{Eu}(\text{CO}_3)_4^{5-}$ at $I = 1 \text{ M}$ (NaClO_4).⁴⁴ The corresponding data, $\log K_3 = 2.65$ for $I = 3 \text{ M}$ (NaClO_4), is indicated in Figure 3. However, according to the carbonate concentrations in the experimental solutions, these two complexes would have been formed at very low concentrations; hence, the stoichiometries as well as the corresponding stability constants are questionable.

The NEA–TDB gave a very interesting and thorough qualitative discussion of each published work on Am(III) and found discrepancies between the equilibrium constants extracted from these studies, even when reinterpretations were attempted.⁵ To resolve these discrepancies, the solubility data were excluded when they used badly characterized solid

(44) Rao, R. R.; Chatt, A. *Radiochim. Acta* **1991**, 54, 181–188.

Table 2. Chemical Conditions of the TRLFS Measurements and Spectral Characteristics of $\text{Cm}(\text{CO}_3)_2^-$ and $\text{Cm}(\text{CO}_3)_3^{3-}$ at Various Temperatures^a

solution label	I_m (mol kg ⁻¹)	$\log [\text{CO}_3^{2-}]$				
		10 °C	25 °C	37 °C	50 °C	70 °C
B2	3.52	-2.69	-2.70	-2.70	-2.70	-2.71
C1	3.48	-1.84	-1.84	-1.84	-1.84	-1.85
C2	3.48	-1.52	-1.53	-1.53	-1.53	-1.54
B4	3.42	-1.30	-1.30	-1.30	-1.30	-1.31
C3	3.49	-1.01	-1.02	-1.02	-1.02	-1.03
C5	3.49	-0.51	-0.51	-0.51	-0.51	-0.52
C6	3.49	0.00	-0.01	-0.01	-0.01	-0.02
C7	4.93	0.30	0.30	0.29	0.29	0.29

	10 °C	25 °C	37 °C	50 °C	70 °C
$\lambda_{\text{max},3}$ (nm)	607.2	607.4	607.6	608.1	608.7
$F_{2,\lambda_{\text{max},3}}$ (a.u)	3730	2380	2010	1830	1050
$F_{3,\lambda_{\text{max},3}}$ (a.u)	20920	17720	15690	15630	12380
$\log K_3(3\text{M})$	1.86 ± 0.15	2.08 ± 0.10	2.10 ± 0.15	2.23 ± 0.15	2.26 ± 0.20

^a $\lambda_{\text{max},3}$ is the wavelength of the maximum of the $\text{Cm}(\text{CO}_3)_3^{3-}$ peak. $F_{2,\lambda_{\text{max},3}}$ and $F_{3,\lambda_{\text{max},3}}$ are the molar intensities at $\lambda_{\text{max},3}$ for $\text{Cm}(\text{CO}_3)_2^-$ and $\text{Cm}(\text{CO}_3)_3^{3-}$, respectively, which were measured in 3 M Na^+ solutions. The $\log K_3$ values were determined by spectral decomposition.

phases¹² and even a reasonably well-characterized $\text{Am}_2(\text{CO}_3)_3(\text{s})$ solid phase that is metastable in carbonate solutions.¹⁰ Hence, the selection of a $\log K_3^\circ$ value was based on a single value from measurements of the solubility of $\text{AmOHCO}_3(\text{s})$ at variable ionic strength,¹¹ giving $\log K_3^\circ = 2.9 \pm 0.5$.⁵ The exclusion of Robouch's data might be questionable because the solubility-controlling solid, $\text{Am}_2(\text{CO}_3)_3(\text{s})$, had been well characterized via its X-ray diffraction pattern. Furthermore, X-ray characterization after two distinct preparation procedures and at different times (pages 51, 57, and 58 in ref 10) showed that, at room temperature, the $\text{Am}_2(\text{CO}_3)_3(\text{s})$ compound was always detected even in chemical conditions where it was metastable; the only detected solid-phase transformation gave $\text{NaAm}(\text{CO}_3)_2(\text{s})$ after 8 weeks in a 1 M Na_2CO_3 solution, while the other possible stable phase $\text{AmOHCO}_3(\text{s})$ was never detected. The $\log K_3$ value was determined to be 2.52 ± 0.14 at $I = 3$ M (NaClO_4) and should be relevant.¹⁰ In the updated NEA–TDB review, thermodynamic data for both $\text{Am}(\text{III})$ and $\text{Cm}(\text{III})$ were considered, and the value of $\log K_3^\circ$ was determined to be 2.1 ± 0.8 to cover all of the selected values.¹⁵ $\text{Cm}(\text{III})$ values were taken from TRLFS studies, $\log K_3^\circ = 2.09 \pm 0.15$ ²³ and $\log K_3^\circ = 2.00$,²⁴ but the TRLFS spectra were interpreted assuming $\text{Cm}(\text{CO}_3)_4^{5-}$ stoichiometry for the limiting complex, while the expected limiting complex should be $\text{Cm}(\text{CO}_3)_3^{3-}$.²² This may very well be the reason that the NEA–TDB selected value, $\log K_3^\circ = 2.1 \pm 0.8$,¹⁵ is different from the value of $\log K_3^\circ$ (0.94 ± 0.24) found in the present work. Finally, we found possible reasons for understanding the discrepancies of the data at 25 °C for f-block trications on the basis of chemical behavior (i.e., for $\text{Ce}(\text{III})$), characterization of the solubility-controlling solid (i.e., for $\text{Am}(\text{III})$), or possible misinterpretations. These statements may be supported by the consistency of the TRLFS results and solubility data obtained at variable temperatures for $\text{Cm}(\text{III})$ and $\text{Am}(\text{III})$, as presented below.

4.3. Carbonate Complexes of $\text{Cm}(\text{III})$ Over 10–70 °C. Temperature cycles were carried out in solutions for which $[\text{CO}_3^{2-}]$ was calculated and reported in Table 2. For each temperature, fluorescence was measured as a function of $[\text{CO}_3^{2-}]$. An example is given in Figure 4 for measurements

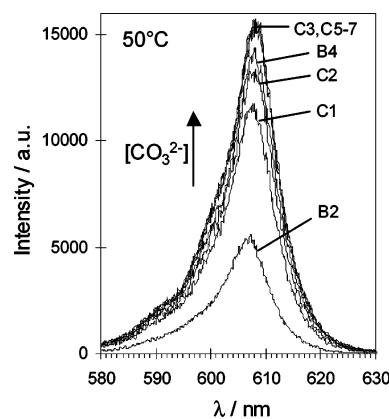


Figure 4. Influence of $[\text{CO}_3^{2-}]$ on the fluorescence spectra measured at 50 °C. The solution labels are indicated on the graphic, referring to Table 2.

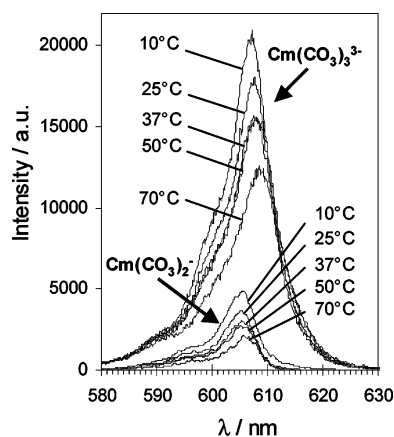


Figure 5. Temperature influence on the fluorescence spectra of $\text{Cm}(\text{CO}_3)_3^{3-}$ as measured in solution C6 (Table 1) and $\text{Cm}(\text{CO}_3)_2^-$ as deduced from spectral decomposition.

at 50 °C. As for experiments at 25 °C, the limiting complex, $\text{Cm}(\text{CO}_3)_3^{3-}$, was detected as the single species in solutions when $[\text{CO}_3^{2-}] > 0.1$ M and dissociated for lower values. As a result, the spectrum recorded for solution C6 (Table 2) corresponds to the one of $\text{Cm}(\text{CO}_3)_3^{3-}$. In addition to a decrease of the fluorescence intensity with increased temperatures, the maximum of the peak was shifted toward the red wavelengths as shown in Figure 5. For a given temperature, the intensity of the spectrum of $\text{Cm}(\text{CO}_3)_2^-$ is about

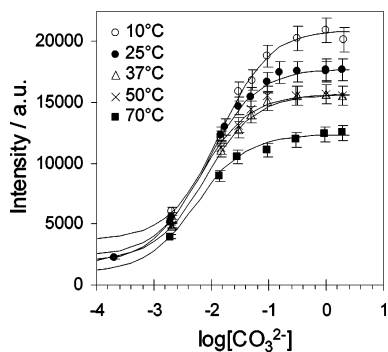


Figure 6. $[\text{CO}_3^{2-}]$ and temperature influences on the fluorescence intensities measured at the wavelength corresponding to the maximum intensity for $\text{Cm}(\text{CO}_3)_3^{3-}$, $\lambda_{\text{max},3}$. The chemical conditions and the parameters ($F_{2,\lambda_{\text{max},3}}$, $F_{3,\lambda_{\text{max},3}}$, and $\log K_3$) for drawing the curves are reported in Table 2.

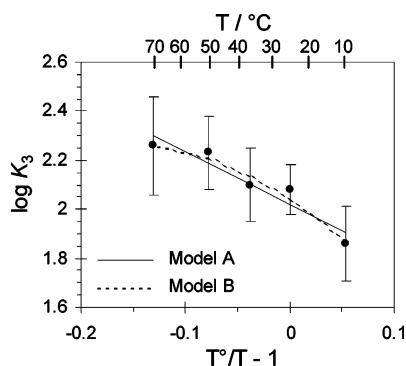


Figure 7. Temperature influence on $\log K_3$ at $I = 3$ M. Symbols and lines correspond to experimental values (Table 2) and fitting curves, respectively. The fitted parameters for Models A and B are reported in Table 3.

four times lower than that of $\text{Cm}(\text{CO}_3)_3^{3-}$, and the shift of the peak is about 2 nm toward the short wavelengths. To display the spectral changes at each temperature, the intensities measured at the wavelength corresponding to the maximum intensity for $\text{Cm}(\text{CO}_3)_3^{3-}$ are plotted over $\log [\text{CO}_3^{2-}]$ in Figure 6, in the same manner as the analysis at 25 °C (Figure 1b). The curves were calculated using eq 1 with the values of $\log K_3$ obtained from the spectral decompositions and spectroscopic parameters for each temperature (Table 2). As was concluded from the results found at 25 °C, a single CO_3^{2-} is exchanged in the dissociation reaction of $\text{Cm}(\text{CO}_3)_3^{3-}$ according to the shape of the curves. Thus, $\text{Cm}(\text{CO}_3)_2^-$ and $\text{Cm}(\text{CO}_3)_3^{3-}$ are still the predominant forms of Cm(III), and only $\log K_3$ is affected by the temperature.

4.4. Effect of Temperature on K_3 and $\Delta_r H_3$. The values of $\log K_3$ for the formation of $\text{Cm}(\text{CO}_3)_3^{3-}$ (Table 2) are plotted as a function of temperature in Figure 7. In the range 10–70 °C, a slight increase of $\log K_3$ was observed. Uncertainties were found to be ± 0.1 – 0.2 , a usual value for the uncertainties associated to measured complexation constants. The dependency of $\log K_3$ with temperature was virtually within uncertainty. Consequently, two models were applied to the experimental data determined at $I = 3$ M as well as to the values extrapolated to $I = 0$. Model A (eq 6) gave a linear correlation and fitted reasonably well the experimental data (Figure 7). The resulting values are $\Delta_r G_3$ -

(298 K) = -11.5 ± 0.2 kJ mol $^{-1}$, $\Delta_r H_3(298 \text{ K}) = 12.2 \pm 2.3$ kJ mol $^{-1}$, and $\Delta_r S_3(298 \text{ K}) = 79 \pm 8$ J mol $^{-1}$ K $^{-1}$. The estimations from Model B (eq 7) are also reported in Table 3. The standard deviation σ of the fit was examined when changing the values of $\Delta_r G_3(298 \text{ K})$, $\Delta_r H_3(298 \text{ K})$, $\Delta_r C_{p3}(298 \text{ K})$, and $\Delta_r S_3(298 \text{ K})$ around the values obtained with Model B. As σ did not increase symmetrically on both sides of the values adjusted with Model B, we determined another set of parameters (Model B'): we assessed the limiting values for which the fit was visually acceptable according to experimental uncertainties, and then we calculated the mean values of each data set. The thermodynamic data obtained with either method B or B' did not significantly differ within their uncertainties. Whether the heat capacity effects were neglected (Model A) or not (Model B), the result was similar values for $\Delta_r G_3$ but somewhat different values for $\Delta_r H_3$ (even if the uncertainty ranges still overlapped) because of the influence of $\Delta_r C_{p3}$ (Table 3). It is not clear whether Model B is meaningful because it assumes a constant $\Delta_r C_{p3}$, while it is not specially expected to be constant for solutes in aqueous solutions: the values fitted for $\Delta_r C_{p3}$ and associated uncertainties are probably only a maximum range of variations, rather than an estimation of its value at 25 °C or even a mean value. One may expect $\Delta_r C_{p3}$ to be small because reaction 2 is isoelectric: it has indeed been proposed that the main contributions to the temperature dependency are the electrostatic interactions and that they should balance out to a large extent.³⁶ Hence, the enthalpy of reaction would be constant with temperature. Thus, Model A is expected to be a relevant approximation for the dependency of $\log K_3$ on temperature. The corresponding thermodynamic constants are therefore considered reliable, but the uncertainties were finally increased to cover the values obtained with the other models (Table 3).

4.5. Solubility Data for Am(III) Between 20 and 70 °C. In this section, solubility results for Am(III) at different temperatures reported in ref 12 are described, followed by a new interpretation of these measurements. Solubility measurements of Am(III) in 4 M NaCl media had been interpreted with the controlling phases $\text{NaAm}(\text{CO}_3)_2(\text{s})$ at 40, 45, 50, and 70 °C, and $\text{AmOHCO}_3(\text{s})$ at 20, 30, 50, 60, and 70 °C.¹² Interestingly, the results showed that, under these conditions, Am(III) was less soluble when the temperature increased. From slope analysis of the solubility curves, equilibrium constants had been determined for the dissolution reactions of each solid compound into the carbonate complexes, AmCO_3^+ , $\text{Am}(\text{CO}_3)_2^-$, and $\text{Am}(\text{CO}_3)_3^{3-}$, at the different temperatures. Values of $\log K_3$ ($\text{Am}(\text{CO}_3)_2^- + \text{CO}_3^{2-} \rightleftharpoons \text{Am}(\text{CO}_3)_3^{3-}$) had been deduced (Table 4), and were corrected for the effect of the ionic medium: from $I = 4$ M NaCl to $I = 3$ M NaClO $_4$ using eqs 4 and 5. These corrections were found to be negligible; typically the $\log K_3$ values were lowered by 0.02 log units regardless of the temperature. These $\log K_3$ values for Am(III) are slightly higher than the ones for Cm(III) (Figure 3). Although a slight increase of $\log K_3$ with increased temperature had been proposed for Am(III),¹² in agreement with the TRLFS results for Cm(III), the scattering of the data did not allow us to

Table 3. Thermodynamic Constants Obtained at 25 °C for $\text{Cm}(\text{CO}_3)_2^- + \text{CO}_3^{2-} \rightleftharpoons \text{Cm}(\text{CO}_3)_3^{3-}$ from K_3 Values (Table 2, Figure 7) Measured at Constant Ionic Strength, $I = 3 \text{ M NaClO}_4$ (Table 2)^a

model ^b	I	$\Delta_r G_3$ (kJ mol ⁻¹)	$\Delta_r H_3$ (kJ mol ⁻¹)	$\Delta_r C_{p3}$ (J mol ⁻¹ K ⁻¹)	$-T^\circ \Delta_r S_3$ (kJ mol ⁻¹)	log K_3	$\Delta_r S_3$ (J mol ⁻¹ K ⁻¹)
A	3	-11.5 ± 0.2	12.2 ± 2.3		-23.7 ± 2.3	2.01 ± 0.04	79 ± 8
B	3	-11.7 ± 0.1	16.4 ± 2.8	-330 ± 180	-28.1 ± 2.8	2.05 ± 0.02	94 ± 9
B'	3	-11.8 ± 0.5	16.6 ± 1.0	-400 ± 300	-28.4 ± 1.1	2.07 ± 0.09	95 ± 4
		-11.5 ± 0.3	12.2 ± 4.4		-23.7 ± 4.7	2.01 ± 0.05	79 ± 16
A	0	-5.0 ± 0.2	9.4 ± 2.4		-14.4 ± 2.4	0.88 ± 0.04	48 ± 8
B	0	-5.2 ± 0.2	13.9 ± 2.9	-350 ± 180	-19.1 ± 2.9	0.91 ± 0.04	64 ± 10
B'	0	-5.1 ± 0.4	14.2 ± 1.7	-300 ± 200	-19.3 ± 1.7	0.89 ± 0.07	65 ± 6
		-5.0 ± 0.3	9.4 ± 4.8		-14.4 ± 6.9	0.88 ± 0.05	48 ± 23

^a The proposed values (bolded) are taken from Model A with increased uncertainty to encompass the values obtained with the other models. ^b A is the constant enthalpy approach; B is the constant heat capacity approach; and B' is the same as B but the best fit was visually decided (see text).

Table 4. Values for log K_3 at Various Temperatures for $\text{Am}(\text{CO}_3)_2^- + \text{CO}_3^{2-} \rightleftharpoons \text{Am}(\text{CO}_3)_3^{3-}$ from Solubility Measurements in 4 M NaCl, taken from Ref 12 and as Reinterpreted in the Present Work

T (°C)	ref 12	this work
20	2.3 ± 0.3	2.0 ± 0.2
30	2.45 ± 0.17	2.0 ± 0.2
30		2.1 ± 0.2
40	2.94 ± 0.14	2.1 ± 0.2
45	2.94 ± 0.10	2.1 ± 0.2
50	2.62 ± 0.14	2.1 ± 0.2
50	2.66 ± 0.13	2.1 ± 0.2
60	2.98 ± 0.24	2.0 ± 0.2
70	2.98 ± 0.17	1.9 ± 0.2
70		2.2 ± 0.2

accurately determine $\Delta_r H_3$ and $\Delta_r S_3$. The uncertainties were obviously too large, probably as a result of solid phase transformations. As the interpretation of these solubility data had only been based on slope analyses and had not been confirmed by any other solid characterization, we tried other possible slope analyses corresponding to other solid compounds that would have controlled the solubility.

The relative stabilities of the solids $\text{AmOHCO}_3(\text{s})$ and $\text{Am}_2(\text{CO}_3)_3(\text{s})$ were determined by P_{CO_2} ,^{5,18} to better estimate this parameter, we corrected the original experimental data for the possible leak of $\text{CO}_2(\text{g})$, particularly at high temperature. Rather than using a mass balance, we recalculated the carbonate speciation on the basis of the electro-neutrality of the solutions, which does not need to assume no exchange of $\text{CO}_2(\text{g})$ with air. The corrections on $[\text{CO}_3^{2-}]$ were only significant for bicarbonate solutions for which P_{CO_2} ranged between 0.001 and 0.02 atm. This corresponds to the conditions at which $\text{Am}_2(\text{CO}_3)_3(\text{s})$, the initial solid, may transform into $\text{AmOHCO}_3(\text{s})$.¹⁸ However, consistently with the kinetic observation of Robouch,¹⁰ theoretical curves better fitted the data assuming $\text{Am}_2(\text{CO}_3)_3(\text{s})$ and $\text{NaAm}(\text{CO}_3)_2(\text{s})$ as relevant phases, with the solid-phase transformation between these two compounds at about 0.01 M CO_3^{2-} for 4 M Na^+ (Figure S1 of the Supporting Information). The corrected measurements were found to be reasonably consistent with this interpretation, whereas the stability of $\text{AmOHCO}_3(\text{s})$, which had been previously considered for the original (uncorrected) experimental data¹² was now even less convincing. A new set of equilibrium constants was determined, particularly values for log K_3 at each temperature (Table 4). These results are clearly different from the original interpretation as shown in Figure 3. Not only are the log K_3 values less scattered but they also appear to be in good

agreement with the TRLFS results for Cm(III) in the range of 20–50 °C; at higher temperature, they are still in agreement, but the solubility results for Am(III) are slightly more scattered. This could be attributed to the crystallographic structures of the solid at 70 °C which may have changed from the beginning to the end of the temperature cycle. Despite the influence of the solid phase on the data, these new results support the formation constants for $\text{Cm}(\text{CO}_3)_3^{3-}$ measured by TRLFS.

4.6. Discussion on the effect of temperature on log K_3 .

The stepwise formation of $\text{Cm}(\text{CO}_3)_3^{3-}$ is an endothermic reaction and is driven by the entropy, since $T^\circ \Delta_r S_3(298 \text{ K})$ is larger than $\Delta_r H_3(298 \text{ K})$ regardless of the model used to interpret the data (Table 3). This observation is consistent with the common trend observed for the complexation of lanthanides and actinides.⁷ The enthalpy of reaction is usually described as the summation of the dehydration energy and the binding energy; desolvation generally overcomes the formation of cation–ligand bonds contributing to positive $\Delta_r H$ and $\Delta_r S$, which is the case for reaction 2. The entropy of the reaction, $\Delta_r S_3$, was indeed found to be positive and contributed in a larger extent to the Gibbs energy of reaction (Table 3). Changes in the hydration of the species probably accompanied the formation of the tricarbonate complex of Cm^{3+} . The dehydration entropy contribution is certainly favorable for reaction 2 and might very well be the most important effect.

In an attempt to compare the thermodynamic constants for carbonate complexation determined in this work with other data, the reactions for the formation of triacetate complexes of Nd^{3+} and UO_2^{2+} were examined as the binding properties of both carbonate and acetate ligands, and the effective charges on the cations ($\sim +3.2$ for UO_2^{2+})⁴⁵ are likely to be nearly similar. $\Delta_r H_3(298 \text{ K}) \approx 3.8 \text{ kJ mol}^{-1}$ and $-T^\circ \Delta_r S_3 \approx -7.3 \text{ kJ mol}^{-1}$ have been determined for the stepwise formation of $\text{Nd}(\text{Ac})_3(\text{aq})$ at $I = 2.2 \text{ mol kg}^{-1}$ (NaClO_4) and 25 °C.⁴⁶ The signs of these thermodynamic parameters are consistent with what was found for the stepwise formation of $\text{Cm}(\text{CO}_3)_3^{3-}$. In contrast, a slightly negative enthalpy change ($\Delta_r H_3 \approx -2 \text{ kJ mol}^{-1}$) was published for the formation of $\text{UO}_2(\text{Ac})_3^-$, although the

(45) Choppin, G. R.; Unrein, P. J. Thermodynamic study of actinide fluoride complexation. In *Transplutonium Elements*; Muller, W., Linder, R., Eds.; North-Holland Publishing Company: Amsterdam, 1976.

(46) Zanonato, P.; Di Bernardo, P.; Bismondo, A.; Rao, L.; Choppin, G. R. *J. Sol. Chem.* **2001**, *30*, 1–18.

values of $\Delta_r H_1(\text{UO}_2\text{Ac}^+)$ and $\Delta_r H_2(\text{UO}_2(\text{Ac})_2(\text{aq}))$ have been found to be positive.⁴⁷ Such changes have been interpreted with different coordination modes of acetate toward the uranyl ion. The third acetate ligand was proposed to be unidentate in contrast to the bidentate coordination of the first and second acetate anions; the coordination is indeed more constrained around UO_2^{2+} since the ligands are roughly in its equatorial plane. Conversely, all of the carbonate anions should act as bidentate ligands toward M^{3+} , and therefore positive enthalpy changes may be expected even for the third stepwise formation reaction. It should be noted that the heat capacity, $\Delta_r C_{p3}$, that was assessed with Model B was negative, whereas the ones measured for reactions of acetate with Nd^{3+} ,⁴⁶ Th^{4+} ,⁴⁸ and UO_2^{2+} ⁴⁷ have been found to be positive in all cases. This supports the assumption that $\Delta_r C_{p3}$ is small for reaction 2 and even negligible over the 10–70 °C range, in agreement with the values from Model A that are proposed here.

The effect of ionic strength on thermodynamic constants was assessed by a similar data treatment of the $\log K_3^\circ$ values at zero ionic strength, calculated for each temperature using eqs 4 and 5. As expected, the complexation constants were lower than those at high ionic strength (as any highly negatively charged species, the limiting complex is more stabilized at high ionic strength); hence, $\Delta_r G_3^\circ$ is higher than $\Delta_r G_3(3 \text{ M})$ (Table 3). The values of $\Delta_r H_3$ and $\Delta_r S_3$ were found to be smaller at zero ionic strength. Applying eqs 8 and 9 to reaction 2 enabled us to calculate $\Delta_r H_3^{\text{ex}}$ and $\Delta_r S_3^{\text{ex}}$ at a given ionic strength, which gave direct insight for how much the thermodynamic functions depend on I . Because $\Delta_r \epsilon_3$ is small and expected to not be temperature dependent, $\Delta_r \log \gamma_3$ (eq 5) and its first derivative (eq 10) can be calculated with a very little influence from the use of fitted parameters. For instance, at $I = 3 \text{ M}$, we obtained $(\partial D(T)/\partial T)_P = (4 \pm 1) \times 10^{-4} \text{ K}^{-1}$ and $\Delta_r \log \gamma_3 = -1.07 \pm 0.05$; hence, $\Delta_r H_3^{\text{ex}}(298 \text{ K}) = 2.7 \pm 0.8 \text{ kJ mol}^{-1}$ and $-T^\circ \Delta_r S_3^{\text{ex}}(298 \text{ K}) = -8.8 \pm 0.9 \text{ kJ mol}^{-1}$. The value of $\Delta_r H_3^{\text{ex}}(298 \text{ K})$ is not zero, but as expected, the effect of I on the

thermodynamic functions is greater for the entropy of reaction than for the enthalpy of reaction. This is again consistent with the stabilization of highly negatively charged complexes such as $\text{Cm}(\text{CO}_3)_3^{3-}$ at high ionic strength.

5. Conclusion

We have demonstrated the reliability of time-resolved laser-induced fluorescence spectroscopy for measuring the stability constants (or equivalently the Gibbs energy of reactions) of the carbonate complexes of Cm^{3+} at various temperatures, which are currently lacking in thermochemical databases. This appeared useful for the system here studied, since TLRFS allowed us to work below the solubility limit, while solubility studies for such systems previously gave scattered thermodynamic data as a result of difficulties in achieving solubility equilibrium. The stepwise formation constant of $\text{Cm}(\text{CO}_3)_3^{3-}$ was measured at 10, 25, 37, 50, and 70 °C. The experimental data at $I = 3 \text{ M}$ could satisfactorily be interpreted neglecting the temperature influence on the enthalpy of the reaction, a classical approximation for such an isoelectric reaction: $\Delta_r H_3(298 \text{ K}) = 12.2 \pm 4.4 \text{ kJ mol}^{-1}$ and $\Delta_r S_3(298 \text{ K}) = 79 \pm 16 \text{ J mol}^{-1} \text{ K}^{-1}$. The dependency of $\log K_3$ was in good agreement with the values for $\text{Am}(\text{III})$ that were obtained from reinterpreted solubility data. As expected, the formation of the limiting tricarbonato complex was found to be entropy driven, probably because of the hydration changes of the species.

Acknowledgment. This work was supported by ANDRA through PhD grant for T.V. and by CEA DEN/DSOE (R&D). The authors would like to thank J.-M. Adnet (CEA Valrho DEN/DRCP/SCPS/LCSE) for providing the ^{244}Cm solution that was used for the preliminary experiments.

Supporting Information Available: Characteristics of the solutions for calibrating the glass electrodes, volume dilatation data, Debye–Hückel term of the SIT formula calculated at various temperatures and ionic strengths, and the graphical interpretation of $\text{Am}(\text{III})$ solubility data at 30 and 70 °C. This material is available free of charge via the Internet at <http://pubs.acs.org>.

IC050214N

(47) Jiang, J.; Rao, L.; Di Bernardo, P.; Zanonato, P.; Bismondo, A. *J. Chem. Soc., Dalton Trans.* **2002**, 1832–1838.

(48) Rao, L. F.; Zhang, Z. C.; Zanonato, P. L.; Di Bernardo, P.; Bismondo, A.; Clark, S. B. *Dalton Trans.* **2004**, 18, 2867–2872.